Journal Pre-proof

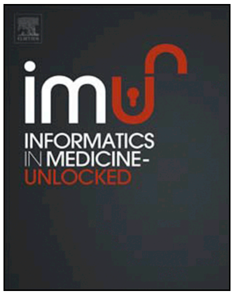

Tetranomial decompression sickness model using serious, mild, marginal, and non-event outcomes

Amy E. King, Laurens E. Howle

PII: S2352-9148(20)30246-X

DOI: https://doi.org/10.1016/j.imu.2020.100371

Reference: IMU 100371

To appear in: *Informatics in Medicine Unlocked*

Received Date: 17 April 2020

Revised Date: 8 June 2020

Accepted Date: 9 June 2020

Tetranomial Decompression Sickness Model using Serious, Mild, Marginal, and Non-Event Outcomes

Amy E. King[a], Laurens E. Howle[a,b,c,d,†]

[a] Department of Mechanical Engineering and Materials Science
Hudson Hall, Research Drive
Duke University
Durham, NC, USA

[b] Department of Radiology
Box 3808 DUMC
Duke University Medical Center
Durham, NC, USA

[c] Division of Marine Science and Conservation
Duke University Marine Laboratory
Beaufort, NC, USA

[d] BelleQuant Engineering, PLLC
7813 Dairy Ridge Road
Mebane, NC, USA

†Corresponding author: laurens.howle@duke.edu, 919.660.5336

Keywords: Decompression sickness, decompression illness, probability, severity, modeling

Abstract

Decompression sickness (DCS) is a condition resulting from reductions in ambient pressure, causing inert gas bubbles in tissues. This work focuses on hyperbaric exposures, specifically DCS resulting from underwater diving. Signs and symptoms of DCS can range from mild skin rashes and joint pain to serious neurological and cardiological malfunction, and even death. Marginal DCS is defined as symptoms associated with DCS that resolve spontaneously without recompression treatment.

There are two categories of decompression modeling used to mitigate risk of DCS: deterministic and probabilistic; neither address DCS symptom severity. Symptom severity is important to U.S. Navy dive planning, as the Navy has different limits for the number allowable cases of mild-symptom DCS and more severe-symptom DCS for a given dive. In this work, a probabilistic model for predicting the tetranomial outcomes of serious, mild, marginal, and no DCS was developed, analyzed, and compared with trinomial and trinomial marginal models from our previous works.

Six variants of exponential-exponential (EE1) and linear-exponential (LE1) models were calibrated with 3,322 air and N_2-O_2 dive exposures detailed in the BIG292 empirical human dive trial data set. Two methods of symptom severity splitting were compared. The log likelihood difference test indicated the LE1 model using a previously-disclosed Type A/B splitting provided the best fit to the empirical dive data of all tetranomial models tested in this work. When comparing this tetranomial model to our previous trinomial and trinomial marginal models using the Pearson chi-squared statistic, we find that the tetranomial and trinomial marginal models' predictions of marginal DCS are not aligned well with the incidence of marginal DCS in the data.

Both the trinomial marginal model in our previous work and tetranomial model presented here are unable to accurately replicate the occurrence of marginal DCS events observed in the BIG292 dataset. These marginal DCS events may hinder model fit during calibration. We recommend the use of the

trinomial model from our previous work, which simultaneously predicts the probability of mild, serious, and no DCS.

Keywords

Decompression sickness, decompression illness, probability, severity, modeling.

1. Introduction

Decompression sickness (DCS) is a condition resulting from a reduction in ambient pressure. This can occur during hyperbaric exposures, such as ascent from a deep-sea dive, and hypobaric exposures, such as ascent to altitude. When ambient pressure is reduced, inert gas which had been inspired, circulated, and dissolved into the body’s blood and tissues at the previous elevated pressure can leave solution, forming bubbles and causing DCS. Signs and symptoms of DCS can range from mild skin rashes and joint pain to serious neurological and cardiological malfunction, and even death [1]. Marginal DCS is defined as symptoms typically associated with DCS that are mild and resolve spontaneously without recompression treatment, such as pain in one joint lasting for less than 60 minutes or pain in two joints lasting less than 30 minutes [2, 3]. Focusing in this work on hyperbaric exposures, DCS is of particular concern for U.S. Navy diver planners, as onset of symptoms can result in premature termination of undersea missions.

The first known decompression model to mitigate the risk of DCS was created by Boycott *et al.* [4] in the early twentieth century, known as the Haldane Model. The Haldane model generated decompression schedules using stage decompression to control the rate of inert gas washout from the body during ascent. This model was deterministic, meaning it predicted that DCS would absolutely occur if the proposed “safe” ascent criteria were violated, and would not occur if these criteria were followed. While this early model did reduce the prevalence of DCS, some divers who complied with the prescribed “safe” decompression schedules still experienced DCS.

Probabilistic decompression modeling was introduced by Weathersby *et al.* [5] and Berghage *et al*. [6] to simulate the variation in DCS onset and severity experienced by divers executing the same dive profile as seen in empirical dive data [2, 3]. Probabilistic decompression algorithms use either gas content or bubble models and survival analysis to generate a probability of DCS for each dive profile [7]. A significant advantage of probabilistic modeling over deterministic modeling is that model parameters can be calibrated with empirical dive data. Probabilistic models used today to predict the probability of the occurrence of DCS do not provide any information about symptom severity. DCS severity predictions would be advantageous as they would allow safety analysis to be conducted on military diving operations.

Both the probability of DCS occurrence and symptom severity are of high concern to the U.S. Navy when planning undersea missions. When planning dives, the U.S. Navy has previously stated that a 2.0% risk of Type I (mild) DCS and a 0.1% risk of Type II (serious) DCS is acceptable [8]. Additionally, U.S. Navy Dive Medical Officers have indicated a low level of concern for marginal DCS [9]. DCS symptom onset can result in premature termination of U.S. Navy diving missions. The addition of the proposed multi-state probabilistic decompression model that predicts both the occurrence and severity of DCS to dive planning would allow dive supervisors to tailor undersea missions to the acceptable level of risk for the divers.

Howle *et al.* [10] introduced a multinomial probabilistic decompression model, which simultaneously predicted the probability of three outcomes for a given dive profile: mild DCS, serious DCS, and no DCS. Howle tested two classifications of DCS cases as mild and serious based on the symptom histories published in the data set used for model calibration [2, 3], one in accordance with current U.S. Navy severity definitions [11] and one novel approach [10, 12]. Howle's trinomial model considered marginal DCS as non-events following previous research on the effectiveness of marginal events in probabilistic model calibration [13, 14]. This trinomial model was compared with a binomial model (predicting full DCS and no DCS outcomes), and it was concluded that the trinomial model provided statistically significant improvement over the binomial model in its ability to fit empirical dive data.

In a companion work, we modified Howle's trinomial model by analyzing the multi-state outcome of full DCS, marginal DCS, and no DCS [15]. Historically, marginal DCS events have been included in probabilistic decompression models as fractionally weighted during model calibration. Originally, marginal events were assigned a weighting of 0.5, indicating they were half as important as a full DCS event during model fitting. This weighting was later reduced to 0.1 when U.S. Navy Medical Officers indicated a low level of concern for marginal DCS, to ensure that marginal DCS cases did not cause undo risk to be associated with particular dives during model calibration [9]. Further research on the impact of fractionally weighted marginal events in probabilistic model fitting has indicated that fractionally weighted marginal DCS events may hinder a model's performance [13, 14]. To address this issue, we developed the aforementioned trinomial marginal model, which considered marginal DCS to be a fully-weighted hierarchical outcome separate from full DCS. This model could not be compared directly with Howle's trinomial model, which classified marginal DCS as nonevents, though we found the inclusion of marginal events in this fashion may have skewed the distribution of predictions on the data. In the present work, we continue the investigation of multinomial probabilistic modeling by optimizing a tetranomial model with mild DCS, serious DCS, marginal DCS, and no DCS outcomes.

2. Methods

2.1 Calibration Data

The model presented in this study was calibrated with the BIG292 standard DCS data set, which is a subset of data presented in two Naval Medical Research Institute (NMRI) reports [2, 3]. The BIG292 data contains 3,322 exposures of air and nitrogen-oxygen diving conducted by the United States, United

Kingdom, and Canadian militaries from 1944-1997. This data set includes the dive profile, dive conditions (wet or dry), inspired gas, and DCS outcome and symptom history for each exposure. The BIG292 data set contains a total of 190 DCS cases and 110 marginal DCS cases resulting from single air, single non-air, repetitive and multilevel air, repetitive and multilevel non-air, and saturation dive types. Marginal DCS is defined as signs or symptoms associated with DCS that persist for a short duration and spontaneously resolve without recompression treatment [2, 3]. The dive data used in this study are de-identified and available to the public in the form of two U.S. government reports, and no IRB approval was required for the present study.

If DCS occurs, the onset time window of DCS symptoms can be characterized by times T_1 and T_2, where T_1 is the last known time a diver was asymptomatic and T_2 is the first known time a diver was definitely experiencing DCS symptoms [16]. In the BIG292 data set, all 190 full DCS cases and 68 of the 110 marginal DCS cases are reported with symptom onset times T_1 and T_2. These symptom onset times can be used in probabilistic DCS modeling to improve model fitting [17]. In our previous work, we found the onset time window provided by T_1 and T_2 are not related to DCS symptom severity, and may actually be biased by the medical surveillance protocol of each dive trial [18].

2.2 DCS Event Severity

DCS cases are categorized into Type I (also called mild or pain-only) or Type II (also called serious or neurological) [8, 11]. A novel method of categorizing DCS cases was proposed by Howle *et al.*, in which the 190 full DCS cases in our calibration data set are classified by perceived severity index (PSI) [10, 12]. These indices for describing DCS symptoms, in order of least to most severe, are: constitutional/nonspecific (dizziness, fatigue, nausea), lymphatic/skin (itching, rash, marbling), pain (ache, joint pain, spasm), mild neurological (paresthesia, numbness, tingling), cardiopulmonary (hemoptysis, dyspnea, cough), and serious neurological (dysfunction of bladder, coordination, mental status).

The dive data published in the two NMRI reports [2, 3] included symptom descriptions for each case of full and marginal DCS, so Howle *et al.* assigned each case a severity index 1-6 [10]. If a case exhibited symptoms corresponding to more than one severity category, the most severe index present was selected.

The traditional categorization of Type I DCS corresponds to constitutional, skin, and pain manifestations, while mild neurological, cardiopulmonary, and serious neurological cases are considered Type II DCS [11]. Howle *et al*. [10] proposed Type A/B splitting, in which Type A DCS includes constitutional, skin, pain, and mild neurological symptoms, while Type B DCS corresponds to cardiopulmonary and serious neurological. The number of DCS occurrences in the BIG292 data set corresponding to each PSI and classified by both Type I/II and Type A/B splitting are summarized in Table 1.

Perceived Severity Index	Type I/II	Type A/B
6 Constitutional/Nonspecific	Type I 152 DCS Occurrences	Type A 170 DCS Occurrences
5 Lymphatic/Skin		
4 Pain		
3 Mild Neurological	Type II 38 DCS Occurrences	
2 Cardiopulmonary		Type B 20 DCS Occurrences
1 Serious Neurological		

Table 1. Classification of BIG292 DCS events according to perceived severity index (PSI) and

corresponding Type I/II and Type A/B splitting.

2.3 DCS Models

Probabilistic DCS models use survival analysis with a gas content or bubble volume model to quantify the risk of DCS occurrence for a given dive profile [7]. Our tetranomial probabilistic models extended the exponential-exponential (EE) and linear-exponential (LE) gas content models described by Thalmann [19], which consist of three stirred, parallel perfused gas compartments. The models in this work were added to our previously developed DCS modeling and optimization system, described in previous work [20, 21].

Twelve probabilistic decompression model variants were tested to determine which model parameters were statistically justified for the tetranomial model. The base model was the EE1 model, which consists of three well-mixed, parallel-perfused compartments. Each compartment exhibits exponential gas kinetics and has a unique half-time. The slowest compartment has a pressure threshold parameter, allowing for greater gas supersaturation before risk accumulation. We also tested two additional variants of this EE1 model – one without any threshold parameter (EE1nt), and one with threshold parameters in all three compartments (EE1 full). Next, we tested the LE1 model, which augments the EE1 model by allowing for a switch between exponential and linear gas kinetics at an optimized crossover pressure in the middle compartment [9, 19]. The two variants of that LE1 model were one without any threshold parameter (LE1nt), and one with both threshold and crossover pressure parameters in all three compartments (LE1 full). A detailed derivation of these models can be found in Ref. [21]. A summary of the free parameters in each model variant can be found in Table 3.

These three EE1 and three LE1 models were tested with Type I/Type II splitting, and again with Type A/Type B splitting, totaling 12 model variants.

2.4 Tetranomial Model

The binomial probability of DCS occurrence, as defined by Weathersby *et al.* [5], is

$$P_{DCS} = 1 - e^{-\vec{g}\cdot\vec{R}} \tag{1}$$

and the probability of DCS not occurring is defined by the law of total probability as

$$P_0 = 1 - P_{DCS} = e^{-\vec{g}\cdot\vec{R}}. \tag{2}$$

In Eqs. (1) and (2), $\vec{g}$ is a vector of each compartment's gain and $\vec{R}$ is a vector containing each compartment's risk information. The risk function is derived from survival analysis and quantifies the gas kinetics in each compartment; a detailed derivation can be found in Refs. [21, 22].

It has been shown that including the DCS symptom onset time information in Eq. (1) can improve a model's performance, and is done by calculating the joint probability of surviving DCS-free until T_1 and experiencing DCS during the onset time window T_1-T_2 [17]. This joint probability can be written as

$$P_{DCS} = P_{0,0\rightarrow T_1} P_{DCS,T_1\rightarrow T_2} = e^{-\vec{g}\cdot\int_0^{T_1}\vec{r}dt}\left(1-e^{-\vec{g}\cdot\int_{T_1}^{T_2}\vec{r}dt}\right), \tag{3}$$

where $P_{0,0\rightarrow T_1}$ is the probability of surviving DCS-free until time T_1 (Eq. (2)), and $P_{DCS,T_1\rightarrow T_2}$ is the probability of DCS occurring between times T_1 and T_2 (Eq. (1)). These equations can be extended to the proposed tetranomial model, in which the probabilities of serious, mild, marginal, and no DCS are all calculated simultaneously. Competitive probabilities, meaning probabilities for each event independent of any other event occurring, are derived from Eq. (1) using fitted scale factors a and b to differentiate between DCS severity:

$$
\begin{aligned}
P_s^c &= 1 - e^{-a(\vec{g}\cdot\vec{R})} \\
P_m^c &= 1 - e^{-\vec{g}\cdot\vec{R}} \\
P_n^c &= 1 - e^{-b(\vec{g}\cdot\vec{R})}.
\end{aligned}
\tag{4}
$$

In Eq. (4), P_s^c, P_m^c, P_n^c are the competitive probabilities of serious, mild, and marginal DCS respectively.

2.5 Competitive and Hierarchical Probabilities

Observed cases of DCS are categorized hierarchically. For example, the diagnosis of serious DCS would take precedence over mild and marginal DCS if mild and/or marginal DCS symptoms were present, and mild DCS takes precedence over marginal DCS. The calculated DCS probabilities in Eq. (4) are defined competitively, and consequently must be converted to hierarchical probabilities to accurately reflect the diagnoses in our dive data. These hierarchical probabilities, labeled with a superscript h, can be calculated from competitive probabilities as the joint probability of the event's independent probability and the probability that the more severe event(s) does not occur:

$$
\begin{aligned}
P_s^h &= P_s^c \\
P_m^h &= P_m^c(1 - P_s^c) \\
P_n^h &= P_n^c(1 - P_s^c)(1 - P_m^c) \\
P_0^h &= 1 - P_s^h - P_m^h - P_n^h
\end{aligned}
\tag{5}
$$

Eq. (5) lists the hierarchical probabilities of serious, mild, marginal, and no DCS occurring calculated from their competitive probabilities. The sum of the probabilities of all events is equal to 1 by the law of total probability. For comparison with [10, 15], we can rewrite Eq. (5) in Howle's compact notation, where a quantity ξ is defined as

$$
e^{-\vec{g}\cdot\vec{R}} = \xi \tag{6}
$$

and

$$\begin{aligned} e^{-a(\vec{g}\cdot\vec{R})} &= \xi^{a} \\ e^{-b(\vec{g}\cdot\vec{R})} &= \xi^{b}. \end{aligned} \tag{7}$$

Eqs. (6) and (7) can be substituted into the hierarchical probabilities in defined Eq. (5):

$$\begin{aligned} P_s^h &= 1-\xi^{a} \\ P_m^h &= \xi^{a}-\xi^{a+1} \\ P_n^h &= \xi^{a+1}-\xi^{a+b+1} \\ P_0^h &= \xi^{a+b+1} \end{aligned} \tag{8}$$

The hierarchical probabilities of serious, mild, and marginal DCS are plotted with increasing hazard function for a single compartment in Figure 1. The probability of serious DCS increases with increasing hazard function, while the probabilities of mild and marginal DCS increase and then decrease. This plot illustrates the masking of less severe DCS events by more severe DCS, i.e. a diver diagnosed with serious DCS may have also been experiencing mild DCS symptoms. We hypothesize that as the risk function increases, it is more likely that the diver will develop serious DCS symptoms and thus more likely to be diagnosed with serious DCS and less likely to be diagnosed with mild or marginal DCS.

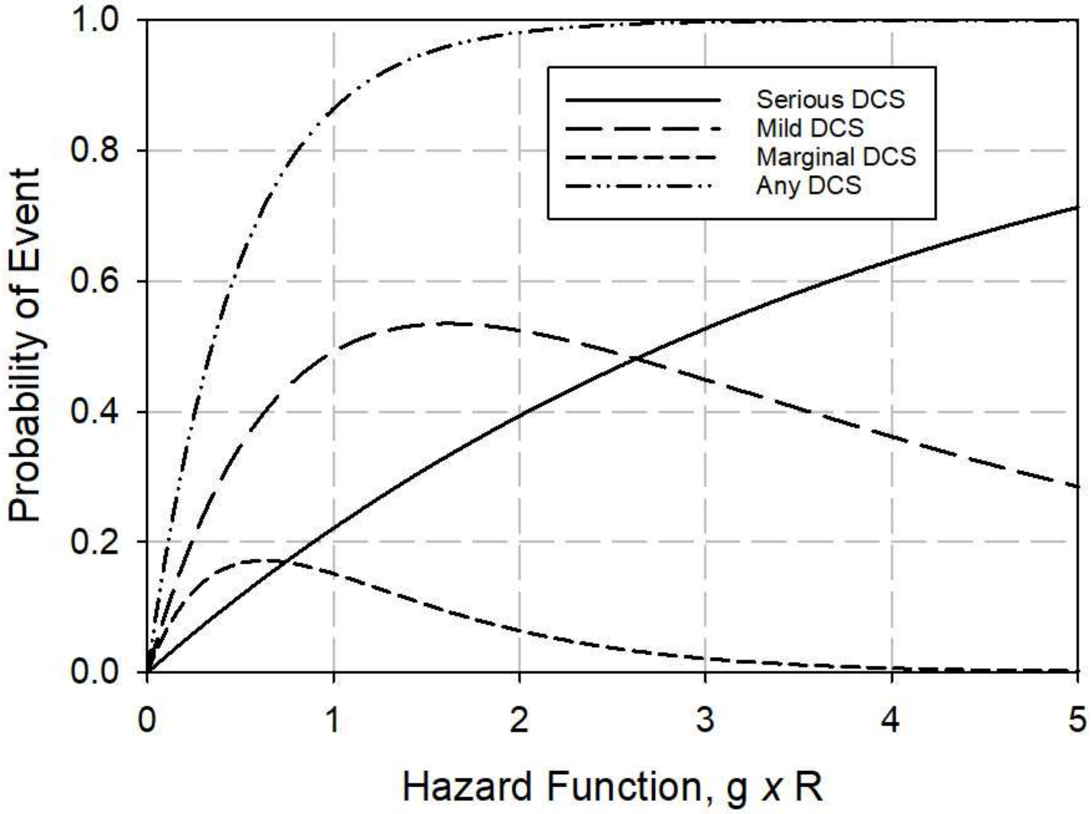

Figure 1. Probabilities of serious, mild, and marginal DCS events with increasing hazard function in the hierarchical model. The masking of mild DCS by serious DCS, and marginal DCS by mild and serious DCS, is illustrated by the decreasing probabilities of mild and marginal DCS events with increasing hazard function. Arbitrary scale factors of $a = 0.25$ and $b = 0.75$ were used to generate this plot.

2.6 Multinomial Likelihood Functions

Probabilistic DCS models are advantageous in their capacity to be calibrated with empirical dive data. To determine optimal model parameters, Weathersby *et al.* [5] used maximization of the likelihood function. Other optimization methods, such as Bayes optimization, have also been used to estimate probabilistic DCS model parameters [23]. Although Bayesian optimization can provide a clearer picture of estimated parameters' uncertainties, it has a high computational cost, so maximum likelihood optimization is used in the present work.

For a binomial model predicting the probabilities of full and no DCS, the log likelihood function is

$$LL_2 = \sum_{i=1}^{N} \ln\left[\left(1-P_{D,i}\right)^{1-\delta}\left(P_{D,i}\right)^{\delta}\right] \tag{9}$$

where $P_{D,i}$ is the probability of DCS occurring for the i^{th} of N total dives, calculated with Eq. (1) or (3). The exponent δ signals the observed outcome of the i^{th} dive, where $\delta=1$ if DCS occurred, and $\delta=0$ if DCS did not occur. This function is optimized to maximize the model's fit to the data.

For our tetranomial model, the hierarchical probabilities defined in Eq. (5) can be used in a multinomial log likelihood function to calculate the fit of the model to the calibration data set:

$$LL_4 = \sum_{i=1}^{N} \ln\left[\left(1-P_{s,i}^{h}-P_{m,i}^{h}-P_{n,i}^{h}\right)^{1-\nu-\mu-\sigma}\left(P_{s,i}^{h}\right)^{\sigma}\left(P_{m,i}^{h}\right)^{\mu}\left(P_{n,i}^{h}\right)^{\nu}\right], \tag{10}$$

where the index i counts over each dive exposure and the dive outcome is expressed with

$$\begin{aligned}
&\sigma=1, \mu=\nu=0 \text{ for serious DCS}\\
&\mu=1, \sigma=\nu=0 \text{ for mild DCS}\\
&\nu=1, \sigma=\mu=0 \text{ for marginal DCS}\\
&\sigma=\mu=\nu=0 \quad \text{for no DCS.}
\end{aligned} \tag{11}$$

The model is optimized with serious, mild, and marginal DCS treated as separate, hierarchical events distinguished by scaling factors.

We can collapse the tetranomial log likelihood function in Eq. (10) to an equivalent trinomial marginal log likelihood function by combining the probabilities of serious and mild DCS to represent full DCS as

$$LL_{43} = \sum_{i=1}^{N} \ln\left[\left(1 - P_{s,i}^{h} - P_{m,i}^{h} - P_{n,i}^{h}\right)^{1-\nu-\mu-\sigma}\left(P_{m,i}^{h} + P_{s,i}^{h}\right)^{\mu+\sigma}\left(P_{n,i}^{h}\right)^{\nu}\right]. \tag{12}$$

In Eq. (12), LL_{43} is the deflated tetranomial-to-trinomial log likelihood function calculated from hierarchical probabilities. We will use this deflated log likelihood to compare the tetranomial model in this work with the trinomial marginal model in our companion work [15].

2.7 DCS Model Optimization and Statistical Methods

The optimal parameters for the tetranomial model were determined with maximization of the tetranomial log likelihood function in Eq. (10). A thorough description of the maximization technique used herein can be found in Ref. [21]. The optimization of Eq. (10) is computationally expensive because some model parameters are nearly collinear. To reduce the number of optimized parameters, Howle previous derived an analytical solution for the optimal compartmental gain values given the rest of the parameter set [20], which can be extended to these multinomial models [10].

All 12 model variants were optimized from 1024 random initial guesses, and the parameter set yielding the maximum log likelihood was chosen for each model. Because these model variants differ in the number of adjustable parameters, their log likelihoods cannot be compared directly, so the log likelihood difference test was used, defined in [7] as

$$\Delta LL_{ij} = \chi^2 = -2\left(LL_i - LL_j\right), \tag{13}$$

where LL_i and LL_j are the log likelihoods of the models being compared. The log likelihood difference comparison value, ΔLL_{ij}, for each model pair can be compared against the Chi-squared distribution value for significant ($p < 0.05$) or highly significant ($p < 0.01$) improvement based on the number of additional degrees of freedom from one model to the other.

The 95% confidence intervals on the optimized parameters were calculated according to Ref. [7]. In this method, the covariance matrix was taken as the negative inverse of the approximate Hessian, and the estimated parameter standard errors were the diagonal components of this covariance matrix. SigmaPlot v14 [24] was used to plot the 95% confidence limits and 95% prediction limits on the models' fits to the data set.

The Pearson Residual group statistic was used to compare each multinomial models' success at predicting each severity of DCS. This statistic was calculated according to Ref. [22], i.e.

$$PR_j = \frac{\left(obs_j - pred_j\right)^2}{pred_j\left(1 - \frac{pred_j}{N_j}\right)} \tag{14}$$

where subscript j indicates the group, obs_j is the number of observed events in the group, $pred_j$ is the number of model-predicted events for that group, and N_j is the total number of exposures in group j. The sum of the Pearson Residuals for all j groups is equal to the Chi-square statistic, χ^2:

$$\chi^2 = \sum_{j=1}^{J} PR_j \quad . \tag{15}$$

In this statistical analysis, the null hypothesis is that the model-predicted incidence of DCS is equal to the incidence of DCS observed in the BIG292 dataset. A high χ^2 value (and corresponding low p-value) indicates that the model's predictions are not consistent with the observed occurrence of DCS in the data.

3. Results

In the subsections below, all 12 optimized model variants are compared and the best performing model chosen using the log likelihood difference test. The best model's predictions on the dive data set are examined, along with the cumulative density function for predicted cases and predicted vs. observed probabilities of DCS. The tetranomial model is then compared with the trinomial and trinomial marginal models from our previous work.

3.1 Tetranomial Model Comparison

For each of the 12 model variants, the parameter sets yielding the best log likelihood were chosen for comparison. The log likelihoods of each splitting type (I/II and A/B) model pair can be compared directly, and for all six pairs, the A/B models performed better than the corresponding I/II models (Table 2). The optimal parameter sets for these six A/B splitting models (EE1, EE1nt, EE1 Full, LE1, LE1nt, and LE1 Full) can be found in Table 3, along with the 95% confidence intervals for the LE1 model.

Model	# DOF	LL	Severity Splitting Type Winner
EE1 NT I/II	8	-1612.30041	EE1 NT A/B
EE1 NT A/B	8	-1581.05407	
EE1 I/II	9	-1589.44908	EE1 A/B
EE1 A/B	9	-1560.50726	
LE1 NT I/II	9	-1609.74076	LE1 NT A/B
LE1 NT A/B	9	-1578.65117	
LE1 I/II	10	-1583.42341	LE1 A/B

LE1 A/B	10	-1549.5327	
EE1 Full I/II	11	-1588.09186	EE1 Full A/B
EE1 Full A/B	11	-1559.70088	
LE1 Full I/II	14	-1586.30942	LE1 Full A/B
LE1 Full A/B	14	-1562.72073	

Table 2. Maximum log likelihood for each of the 12 models optimized from 1024 random initial guesses. Each of the six models (EE1, EE1nt, EE1 Full, LE1, LE1nt, and LE1 Full) was tested with both Type I/II and Type A/B DCS severity splitting. For each of these six models, the log likelihoods of Type I/II and Type A/B splitting can be compared directly to determine which splitting method yields the best model performance.

	EE1nt	EE1	LE1nt	LE1	EE1 Full	LE1 Full
$1/k_1$ (min)	2.295	4.957	3.001	3.496 ± 0.1510	7.802	1.585
$1/k_2$ (min)	245.9	267.6	211.5	63.83 ± 22.86	496.6	578.2
$1/k_3$ (min)	619.6	619.2	607.8	548.1 ± 42.89	149.4	151.0
g_1 (min^{-1})	1.212E-03	3.767E-04	7.665E-04	7.138E-04 ± 4.337E-04	3.743E-04	1.085E-03
g_2 (min^{-1})	4.222E-04	4.719E-04	3.458E-04	9.036E-05 ± 2.603E-05	1.110E-03	5.991E-04
g_3 (min^{-1})	2.032E-04	1.363E-03	2.369E-04	1.049E-03 ± 2.129E-04	1.226E-04	3.461E-04
PXO_1 (fsw)	∞	∞	∞	∞	∞	2.429
PXO_2 (fsw)	∞	∞	0.2897	0.07471 ± 0.01127	∞	4.821
PXO_3 (fsw)	∞	∞	∞	∞	∞	2.708
Thr_1 (fsw)	0	0	0	0	0.07158	0.1220

Thr_2 (fsw)	0	0	0	0	0.1127	0.08404
Thr_3 (fsw)	0	0.2185	0	0.1202 ± 0.01134	-0.06614	-0.02619
a	0.1134	0.1087	0.1124	0.1127 ± 0.01552	0.1235	0.1250
b	0.6756	0.6489	0.6869	0.6981 ± 0.01142	0.7173	0.6000
P(N)	106.83	100.99	107.1	105.83 ± 12.57	102.46	93.11
P(M)	167.41	167.88	165.31	163.2 ± 20.78	153.45	165.27
P(S)	19.72	19.23	19.31	19.31 ± 3.566	19.87	21.6
LL_4	-1581.05	-1560.51	-1578.65	-1549.53	-1559.70	-1562.72

Table 3. Optimal model parameters for all EE1 and LE1 model variants. All model variants in the above table used Type A/B splitting. 95% confidence intervals are given for the LE1 model parameters, which provided the best fit to the BIG292 data set.

The comparisons between the six A/B model variants, which differ in the number of degrees of freedom, were performed with the log likelihood difference test. These log likelihood difference test values (ΔLL_{ij}) can be found in Table 4 for all A/B splitting models, and the Chi-squared distribution values for one to six additional degrees of freedom are in Table 5. In Table 4, the number of adjustable parameters for each model is listed in parenthesis. The log likelihood difference value between each model pair is listed in the corresponding row-column intersection. Reading down a column compares that column's model to models with less degrees of freedom, and reading across a row compares that row's model with models having more degrees of freedom. A bold value indicates the column model provides significant improvement ($p < 0.05$) over the row's model, and a bold and underlined value indicates the column model provides highly significant improvement ($p < 0.01$) over the row's model.

We can see that the use of one pressure threshold parameter is justified, as the EE1 and LE1 provided highly significant improvement over the EE1nt and LE1nt respectively. The crossover pressure parameter enabled the LE1 model to perform significantly better than the EE1 model. However, the EE1 Full and LE1 Full models did offer significant improvement over the EE1 and LE1 models respectively, so the addition of threshold and crossover pressure parameters to all compartments is not justified. We can conclude that the LE1 model provided the best fit to our data, as the LE1 model provided highly significant improvement over the EE1, EE1nt, and LE1nt models. Models with more adjustable parameters than the LE1 (the EE1 Full and LE1 Full) did not offer any improvement. Therefore, all following discussion will pertain to the LE1 model with Type A/B splitting.

	EE1nt (8)	EE1 (9)	LE1nt (9)	LE1 (10)	EE1 Full (11)	LE1 Full (14)
EE1nt (8)	-	**41.094**	**4.806**	**63.043**	**42.706**	**36.667**
EE1 (9)		-	-36.288	**21.949**	1.613	-4.427
LE1nt (9)			-	**58.237**	**37.901**	**31.861**
LE1 (10)				-	-20.336	-26.376
EE1 Full (11)					-	-6.040
LE1 Full (14)						-

Table 4. Log likelihood difference comparison for all models using Type A/B splitting. Each model's number of adjustable parameters is listed in parenthesis. The log likelihood difference value between any two of the six models is located in the corresponding row-column intersection. Values in bold indicate the column model provides significant improvement (p < 0.05) over the row model, and bold and underlined values indicate the column model provides highly significant improvement (p < 0.01)

over the row model.

Δ DOF	p<0.05	p<0.01
1	3.841	6.635
2	5.991	9.210
3	7.815	11.345
4	9.488	13.277
5	11.070	15.086
6	12.592	16.812

Table 5. Chi-squared distribution values for 0.95 (p<0.05) and 0.99 (p<0.01) based on the number of additional degrees of freedom.

The observed probabilities of DCS in the data set and the LE1 tetranomial model's predicted probabilities of DCS are plotted in Figure 2 for marginal (black diamonds, top right), mild (gray circles, top left), serious (white triangles, bottom) DCS. This plot was generated by first sorting the model's per-dive exposure predictions by the probability of no DCS. These per-dive predictions were then placed in bins with equal numbers of observed serious, mild, or marginal DCS cases. For this plot, we used 10 bins of 17 mild DCS outcomes each, 5 bins of 4 serious DCS outcomes, and 5 bins of 22 marginal DCS outcomes. The predicted probabilities of DCS were calculated as the sum of the model's per-dive exposure predictions for that DCS severity divided by the total number of exposures in the bin. The observed probabilities of DCS were calculated as the number of observed DCS outcomes in the bin divided by the total number of dive exposures in the bin. The linear fits for the serious, mild, and marginal DCS data points were plotted ($r^2_{serious} = 0.14$, $r^2_{mild} = 0.65$, and $r^2_{\text{marginal}} = 0.80$), along with the 95% confidence and 95% prediction bands. The line of identity was also plotted (black line). If a model's predictions were perfectly aligned with the data set, all points in this plot would fall on the line of identity. Like the trinomial model in our companion work [15], the marginal DCS data points are less scattered than that of serious and mild DCS. The mild DCS model predictions align the closest with the data set, as the mild DCS linear fit line aligns closer to the line of identity than that for serious or marginal DCS.

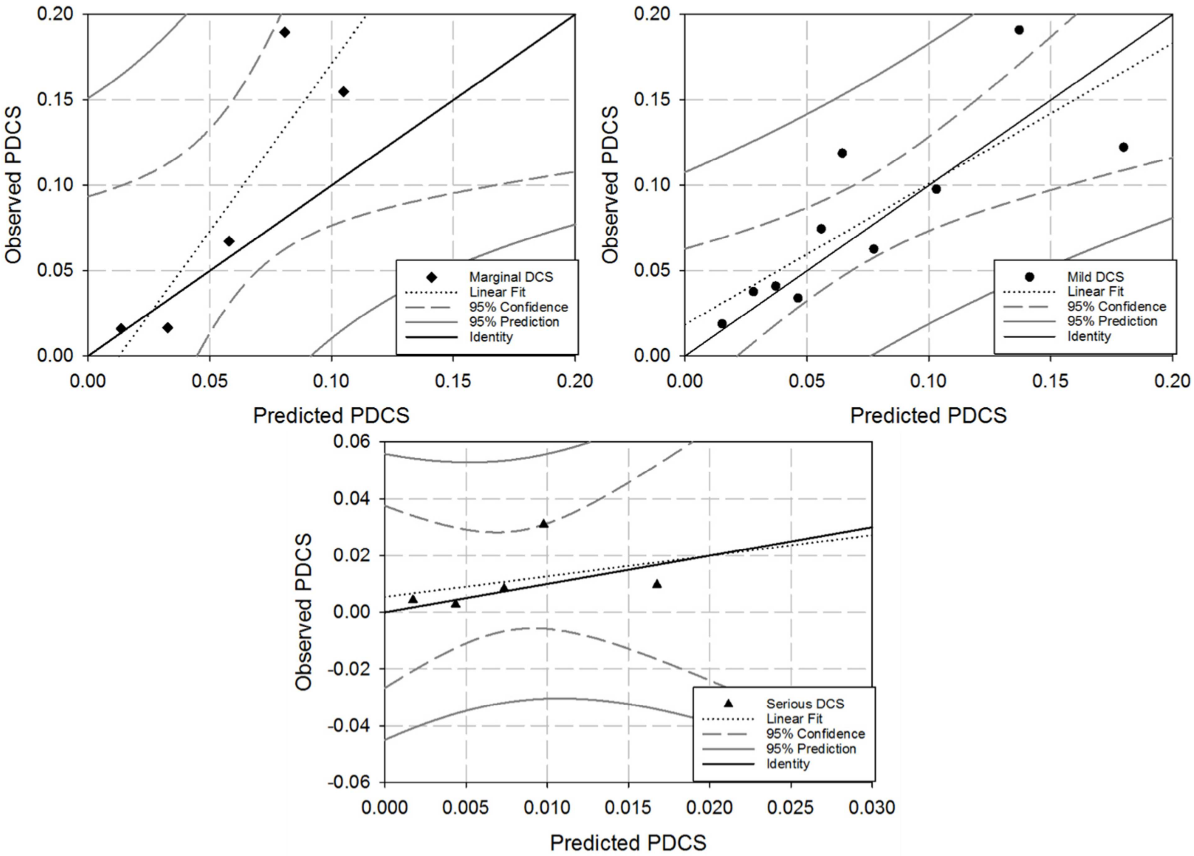

Figure 2. Tetranomial LE1 observed probabilities of DCS vs. predicted probabilities of DCS These probabilities are plotted with a linear fit ($r^2_{marginal} = 0.80$, $r^2_{mild} = 0.65$, and $r^2_{serious} = 0.14$) and the 95% confidence and 95% prediction bands.

3.2 Predictions on Data

The tetranomial LE1 model's predicted DCS outcomes and the observed DCS cases in the data can be found in Table 6. The dive data is separated by dive type, which includes single air, single non-air, repetitive and multilevel air, repetitive and multilevel non-air, and saturation diving. The 95% confidence intervals are listed for the model's total predictions of serious, mild, marginal, and any DCS. These predictions do match the observed number of cases within 95% confidence. From Table 6, we can see that the model underpredicts mild, serious, and marginal DCS occurrence for single air diving.

		Observed DCS				LE1 AB Tetranomial Predicted DCS			
	Exposures	Mild	Serious	Marginal	Total	Mild	Serious	Marginal	Total
Single Air									
EDU885A	483	27	3	0	30	19.77	2.29	13.24	35.3
DC4W	244	7	1	4	12	4.11	0.47	2.81	7.39
SUBX87	58	0	2	0	2	0.14	0.02	0.10	0.26
NMRNSW	91	4	1	5	10	3.88	0.45	2.59	6.92
PASA	72	4	1	2	7	1.87	0.21	1.27	3.35
NSM6HR	57	3	0	2	5	3.10	0.36	2.05	5.51
Rep&Mult Air									
EDU885AR	182	11	0	0	11	8.42	0.98	5.60	15
DC4WR	12	3	0	0	3	0.66	0.08	0.44	1.18
PARA	135	6	1	3	10	6.98	0.81	4.62	12.41
PAMLA	236	9	4	12	25	14.05	1.64	9.25	24.94
Single Nonair									
NMR8697	477	9	2	18	29	11.00	1.26	7.48	19.74
EDU885M	81	4	0	0	4	2.17	0.25	1.48	3.9
EDU1180S	120	9	1	0	10	5.07	0.59	3.38	9.04
Rep&Mult Nonair									
EDU184	239	11	0	0	11	10.17	1.18	6.79	18.14
PAMLAOD	134	5	1	0	6	5.92	0.68	3.98	10.58

PAMLAOS	140	5	0	3	8	4.28	0.49	2.89	7.66
EDU885S	94	4	0	0	4	2.60	0.30	1.77	4.67
Saturation									
ASATEDU	120	11	2	27	40	14.70	1.80	9.05	25.55
ASATNMR	50	1	0	0	1	4.12	0.49	2.66	7.27
ASATNSM	132	18	0	21	39	22.31	2.80	13.16	38.27
ASATARE	165	19	1	13	33	17.88	2.16	11.22	31.26
Totals	*3322*	*170*	*20*	*110*	*300*	*163.2 ± 20.78*	*19.31 ± 3.566*	*105.83 ± 12.57*	*288.34 ± 24.5*

Table 6. DCS occurrences and tetranomial model predictions for the BIG292 data set.

The imbalance in the distribution of marginal DCS events in the data is evident when considering saturation diving. More than half of the marginal DCS events (55%) in the data set occur from saturation diving, though the entire data set is comprised of only 3% marginal events and 14% saturation dives. In Table 6, we can see that the tetranomial model does not reproduce this skew in observed marginal DCS cases, as the model predicts only 33% of marginal cases occurring from saturation diving.

3.3 Tetranomial Model vs. Trinomial Marginal Model

The model parameters used in the trinomial marginal LE1 model along with model performance analysis can be found in Ref. [15]. We can calculate the tetranomial model's equivalent trinomial marginal log likelihood using Eq. (12). For the optimized tetranomial LE1 model parameter set, $LL_{43} = -1485.4$, which is nearly identical to the optimal trinomial marginal LE1 log likelihood found in [15]. This indicates that the performance of the tetranomial model is on par with the trinomial marginal model when using the BIG292 data set. This is likely because both models optimized to nearly identical parameter sets.

The shift in predicted dive exposure probabilities between the trinomial marginal and tetranomial models is plotted in Figure 3. In Figure 3, the trinomial marginal and tetranomial models' predicted probabilities for full DCS are plotted for all full observed DCS cases (gray circles), predicted probabilities of marginal DCS for observed marginal DCS cases (white diamonds), and predicted probabilities of no DCS for observed no DCS cases (gray squares). All these data points fall close to the line of identity, indicating that these models make nearly identical predictions on the data set. The slope of the linear fit to the full DCS data points is 0.9978 ($r^2 > 0.9999$), for marginal DCS data points is 1.000 ($r^2 = 1.000$), and for no DCS data points is 0.9985 ($r^2 > 0.9999$). These slopes approximate the probability shift between the two models, i.e. $P_{tet,\,full} \approx P_{tri\_m,\,full}$ and $P_{tet,\mathrm{marg}} \approx P_{tri\_m,\mathrm{marg}}$. The tetranomial and trinomial marginal models' agreement in hierarchical probabilities for each DCS cases is a result of both models optimizing to nearly identical parameter sets, so one model does not offer significant performance improvement over the other on this data set.

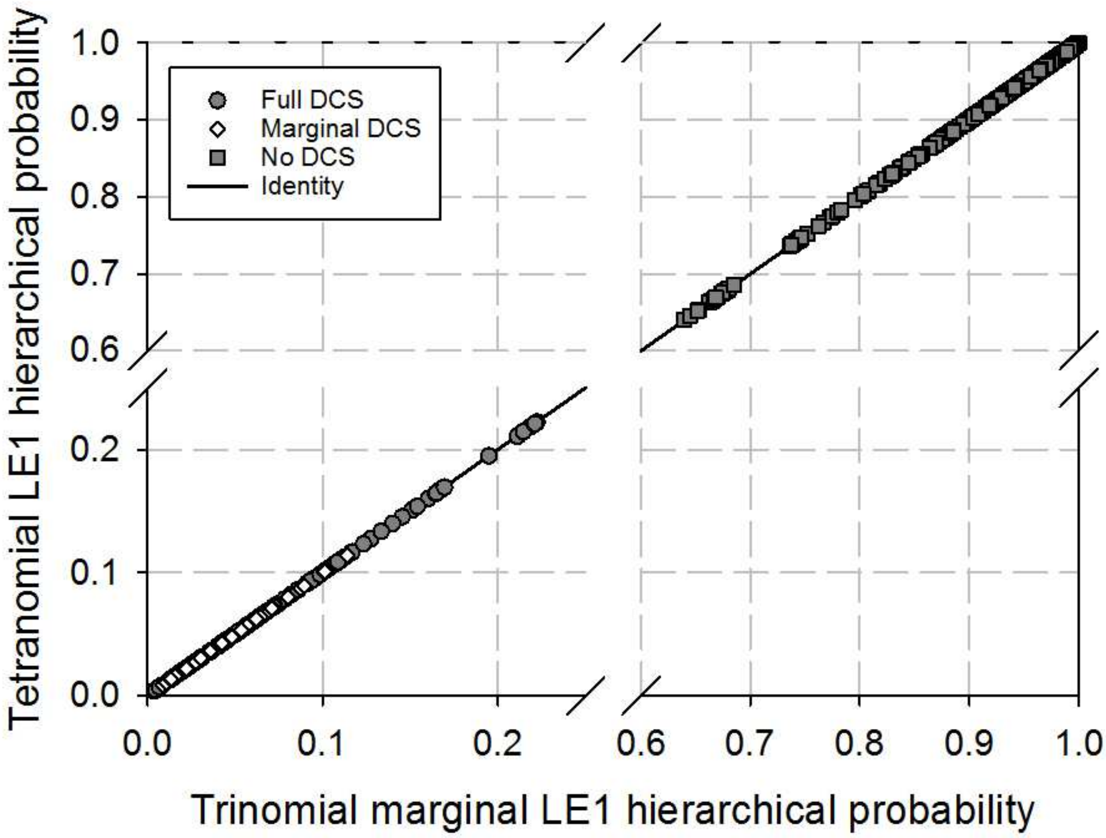

Figure 3. Trinomial marginal to tetranomial probability shift. For dives that resulted in full DCS, the sums of the tetranomial predicted probabilities of serious and mild DCS are plotted against the trinomial marginal predicted probability of full DCS (gray circles). For dive exposures that resulted in marginal DCS and no DCS, the tetranomial model predicted probabilities of marginal (white diamonds) and no DCS (gray squares) respectively are compared with that of the trinomial marginal model.

3.4 Tetranomial Model vs. Trinomial Model

The shift in predicted dive exposure probabilities between the trinomial and tetranomial models is plotted in Figure 4. The model parameters used in this trinomial LE1nt model can be found in [10]. Both models use DCS Type A/B splitting (see Table 1). In Figure 4, the trinomial and tetranomial models' predicted probabilities of mild DCS for dive exposures that resulted in mild DCS are plotted with gray circles, and likewise for serious DCS in white triangles. The trinomial model's predicted probabilities of no DCS and the tetranomial model's predicted probabilities of no- and marginal DCS for dive exposures that did not result in full DCS are plotted with gray squares. The mild DCS and serious DCS data points that fall above the line of identity indicate the tetranomial model predicted a greater probability of occurrence of DCS for those exposures than the trinomial model, and the no DCS points that fall below the line of identity indicate the tetranomial model predicted a lower probability of no DCS for those exposures compared with the trinomial model.

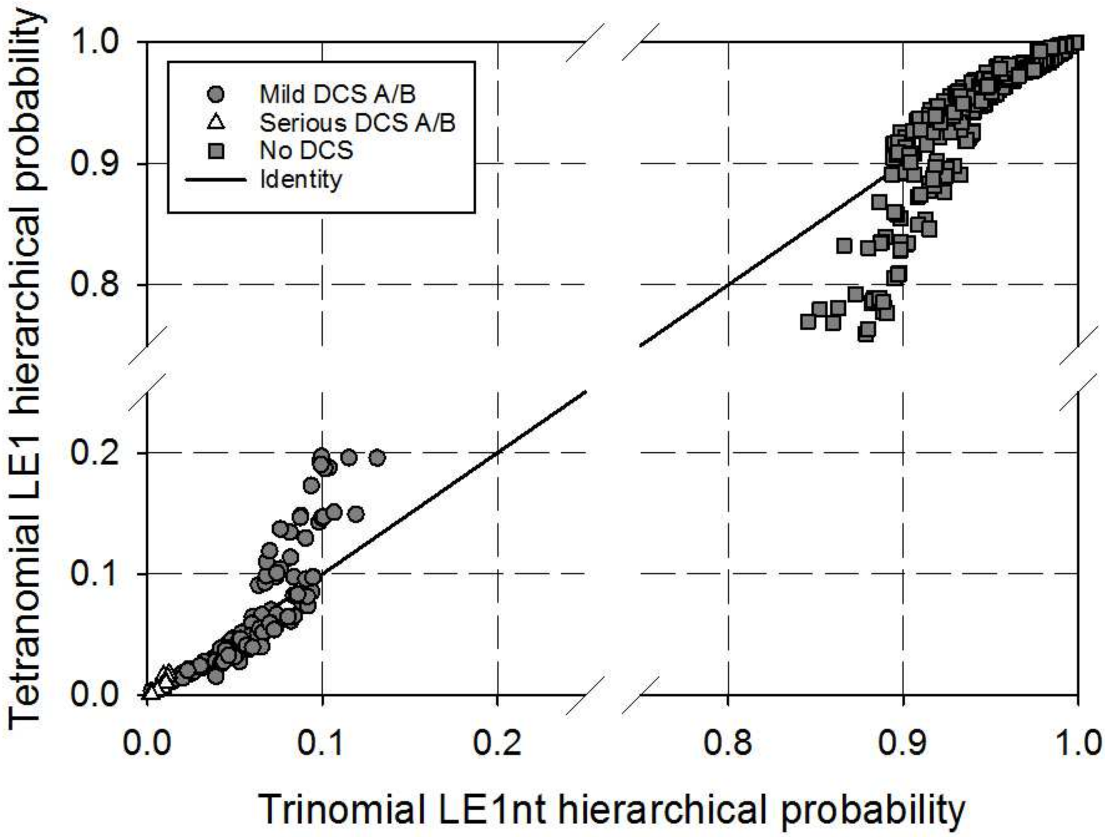

Figure 4. Trinomial to tetranomial probability shift. For dives that resulted in mild or serious DCS, the tetranomial model predicted probabilities of mild or serious DCS are plotted against that of the trinomial

model. For dives that resulted in no DCS (including marginal DCS), the sum of the predicted probabilities of marginal and no DCS for the tetranomial model are compared with the trinomial model's predicted probabilities of no DCS.

The slope of the linear fit to the mild DCS data points is 1.720 ($r^2 = 0.7358$) and the slope of the linear fit to the serious DCS data points is 1.228 ($r^2 = 0.7250$). The line of linear fit to the no DCS points has a slope of 1.352 ($r^2 = 0.7333$). All three sets of data points have similar amounts of scatter, as all have an r^2 value of approximately 0.73. Using these slopes to approximate the trinomial to tetranomial probability shift, $P_{tet,mild} \approx 1.720 P_{tri,mild}$ and $P_{tet,ser} = 1.228 P_{tri,ser}$. Thus, the tetranomial model predicts a greater probability of mild/serious DCS for some mild/serious DCS cases and a lower probability of no DCS for some no DCS cases when compared with the trinomial model.

3.5 Cumulative Density Function

Cumulative density functions (CDF) can be used to visually inspect the DCS symptom onset time agreement between a model's predictions and empirical data. A probabilistic DCS model that performs well on the dataset would produce a CDF that closely replicates that of the data. An in-depth analysis of the BIG292 data set density function was performed in our previous work [18], and it is important to note that the DCS symptom onset times reported in the data may have been biased by the medical surveillance protocol.

The cumulative density functions for the mild, serious, and marginal DCS BIG292 data are plotted in Figure 5 as the solid black curve, solid gray curve, and dashed gray curve respectively. The dashed black line represents the cumulative density function for the tetranomial model's predictions of all DCS types, as scaling factors are used by the model to delineate these severities and thus their cumulative density functions fall on the same curve.

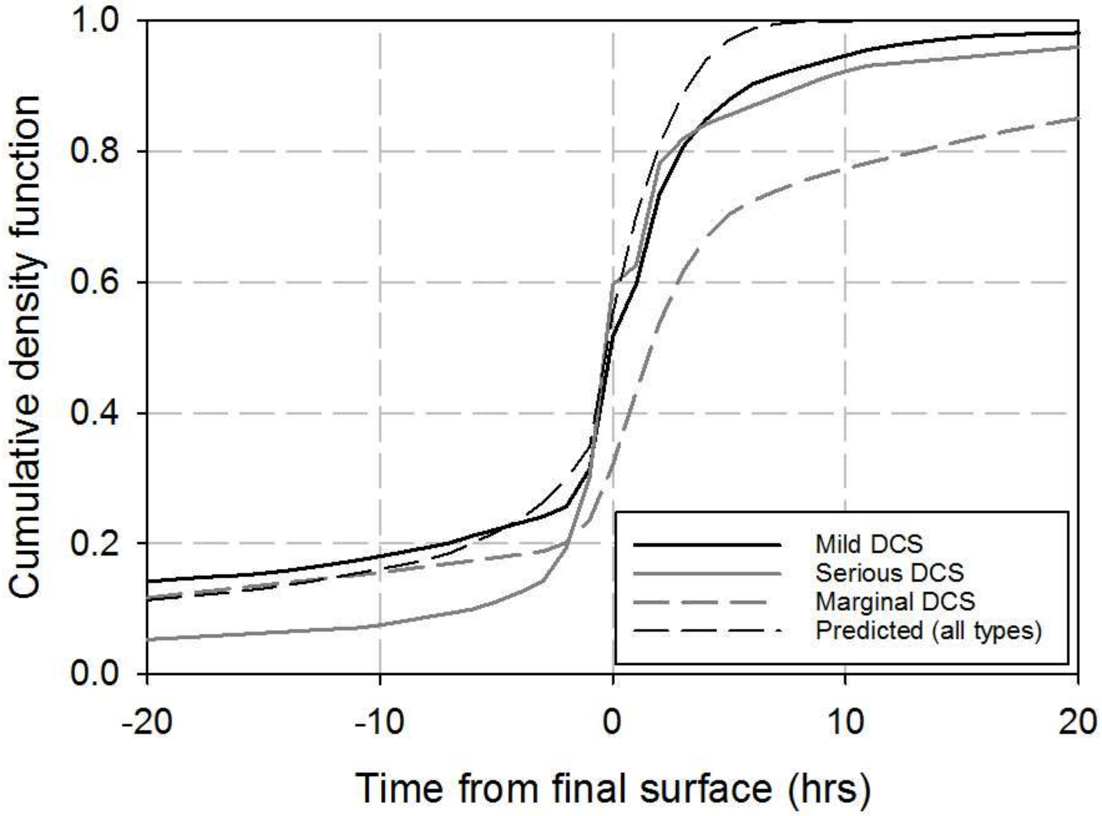

Figure 5. Tetranomial cumulative density function. Mild DCS (black, solid curve), serious DCS (solid, gray curve), and marginal DCS (dashed, gray curve) cases are shown for the BIG292 dive data set. The cumulative density functions for predicted mild, serious, and marginal DCS fall on the same curve (black, dashed).

The tetranomial model's predicted CDF indicates the model most severely over-predicts serious DCS prior to surfacing, then over-predicts the onset of all severities of DCS immediately after surfacing. The tetranomial model's onset time predictions are closely aligned with the marginal DCS cases' onset times until approximately 7 hours prior to surfacing. After surfacing, the marginal DCS data CDF lags behind the mild and serious DCS curves, as the 42 of 110 marginal DCS cases reported without onset times were assigned T_2, or the first known time the diver was experiencing symptoms, at the studies' right-censored times (24 or 48 hours). Because the onset time windows for these 42 marginal cases are imprecise, the tetranomial model's predicted CDF's inability to replicate late onset for marginal cases may not indicate an issue with the model.

3.6 Pearson Residual

The chi-square values calculated from the Pearson Residual of each dive type according to Eqs. (14) and (15) for the binomial and trinomial LE1nt models in Ref. [10], the trinomial marginal LE1 model in Ref. [15], and the tetranomial LE1 model presented in this work can be found in Table 7. It is evident from Table 7 that the trinomial marginal model's and the tetranomial model's predictions of marginal DCS do not align with the observed incidence of marginal DCS, because these groups have a high χ^2 value (and corresponding low p-value).

	Number of DOF	Pearson Residual Full DCS	Pearson Residual Mild DCS	Pearson Residual Serious DCS	Pearson Residual Marginal DCS
Binomial LE1nt [10]	7	8.465 p=0.294			
Trinomial LE1nt [10]	8		8.421 p=0.393	4.527 p=0.807	
Trinomial Marginal LE1 [15]	9	12.270 p=0.199			36.568 p=0.000031

Tetranomial LE1	10		7.597 p=0.668	9.246 p=0.509	36.612 p=0.000066

Table 7. Pearson Residual group statistic (χ^2) and corresponding p-value calculated for each model's predictions of DCS incidence. A high χ^2 value (and corresponding low p-value) indicates that the model's predictions are not consistent with the observed occurrence of DCS in the data.

4. Discussion

The tetranomial model presented here serves as a continuation of the trinomial LE1nt model published by Howle *et al.* [10] and the trinomial marginal LE1 model explored by King *et al.* [15]. All model formulation and analyses were conducted in accordance with those works. In this Discussion section, we will compare all three models.

In this work, we optimized six tetranomial model variants: EE1, EE1nt, EE1 Full, LE1, LE1nt, and LE1 Full. These model variants were tested with both Type I/II and Type A/B splitting, and the Type A/B splitting models outperformed all their corresponding Type I/II splitting models. The log likelihood difference test was used to determine that the LE1 model, with a pressure crossover parameter in the second compartment and a pressure threshold parameter in the third compartment, provided the best fit to the BIG292 data set.

The tetranomial LE1 model predicted the distribution and onset of mild DCS cases better than that of serious and marginal DCS. In Figure 2, the linear fit line for the mild DCS data is closest to the line of identity, and in Figure 5, the predicted CDF is follows closest to the mild DCS curve when compared with serious and marginal DCS. These figures also illustrate that the model is least accurate in predicting both the distribution of marginal DCS cases within the data set and their onset times. These graphical results are verified in Table 7, as the Pearson Residual Chi-squared value is lowest for mild DCS, followed closely by serious DCS. Howle's trinomial model does not follow this trend, and predicts serious DCS more accurately than mild DCS (Table 7). All three models' CDFs indicate they are able to accurately predict the onset of serious and mild DCS around the time of surfacing (Figure 5, [10, 15]).

The high Pearson Residual Chi-squared value for marginal DCS indicates that both the trinomial marginal and tetranomial models' predictions are not aligned with the incidence of marginal DCS in the BIG292 data set. The distribution of marginal DCS cases in the BIG292 data set is skewed towards saturation diving, as 55% of the BIG292 marginal cases occur from saturation diving, and saturation diving only constitutes 14% of the total data. Both the trinomial marginal and the tetranomial LE1 models are unable to reproduce this skew, and only predict 34% of marginal DCS cases occurring from saturation diving. In addition, the marginal cases with right-censored T_2 times may not accurately reflect the true symptom onset times. Neither the trinomial marginal nor the tetranomial models predict the onset time delay created by this right-censoring (Figure 5, [15]). This may not indicate an inherent flaw in these models' ability to predict marginal DCS, rather points to an issue with potentially inaccurate data.

When comparing this tetranomial LE1 model with the trinomial marginal LE1 model in Figure 3, all data points fall close to the line of identity. Both models make nearly identical predictions on the data set. In Table 6, the sums of the tetranomial model's mild DCS and serious DCS predictions for each dive type are nearly equivalent to the trinomial marginal model's predictions for full DCS in Ref. [15]. Both models optimized to nearly identical parameter sets. When using the tetranomial model's equivalent trinomial marginal log likelihood to compare these two models, no clear winner emerges.

The optimal tetranomial model parameter set is quite different from the trinomial model's optimal parameters Ref. [10], which considers marginal DCS events as non-events. In Figure 4, the tetranomial model predicts a higher probability of mild and serious DCS than the trinomial model for some mild and serious DCS cases, and a lower probability of no DCS than the trinomial model for some no DCS cases. The increase in scatter of these data points when compared with Figure 3 illustrates the difference in optimal parameter sets which alters each models' predictions. It could be argued that the tetranomial model would generate more conservative "safe" ascent criteria than the trinomial model, as the tetranomial model predicts increased probabilities of DCS and decreased probabilities of no DCS than the trinomial model.

When the trinomial model was compared with a binomial model in [10], the probability shift plot showed a similar trend as Figure 3 and both optimal parameter sets were nearly identical. However, the trinomial model's equivalent binomial log likelihood indicated the trinomial model performed highly significantly better than the binomial model on the BIG292 data set.

5. Conclusion

The tetranomial model explored in this work simultaneously predicts the hierarchical probabilities of serious, mild, marginal, and no DCS. The derivation of these hierarchical probabilities and the multinomial log likelihood function used during model calibration are extensions of the previous Howle *et al*. work [10].

Both the trinomial marginal model in Ref. [15] and tetranomial model presented here are unable to accurately replicate the occurrence of marginal DCS events observed in the BIG292 dataset. These marginal DCS events may hinder model fit during calibration, there is a concentration in marginal DCS outcomes resulting from saturation diving. A reviewer suggested modifying the tetranomial model presented in this work by optimizing separately on bounce diving and saturation diving data. Future work could include the creation of two tetranomial models, one that predicts serious, mild, marginal, and no DCS for bounce diving, and one that predicts serious, mild, marginal, and no DCS for saturation diving, with the goal of mitigating the bias the BIG292 dataset presents with marginal DCS outcomes.

The trinomial LE1nt model in [10] demonstrated highly significant improvement over the binomial LE1nt model, both considering marginal DCS as non-events. Using the Pearson's χ^2 as a metric, we find that the trinomial LE1nt model's predictions are most closely aligned with the incidence of observed DCS in the data. We therefore recommend the use of the trinomial LE1nt model from Ref. [10] with the event categories of serious, mild, and no-DCS, Type A/B severity splitting, and marginal events scored as non-events. This trinomial probabilistic model can be used to generate dive schedules specific to symptom severity, to better tailor dive missions to the acceptable level of risk for the divers.

Acknowledgements

This material is based upon work supported by the National Science Foundation Graduate Research Fellowship under Grant No. DGE-1644868 and by the U.S. Navy, Naval Sea Systems Command under contracts #N00024-13-C-4104 and #N00024-17-C-4317. Any opinion, findings, and conclusions or recommendations expressed in this material are those of the authors and do not necessarily reflect the views of the National Science Foundation or the U.S. Navy. Computational resources were provided by BelleQuant Engineering, PLLC. Neither funding agency nor the commercial entity played any role in designing this study, data collection and analysis, decision to publish, interpreting the results, or writing the manuscript.

Conflict of Interest Statement

No authors have any conflicts of interest to disclose.

References

[1] R.E. Moon, R.D. Vann, P.B. Bennett, The Physiology of Decompression Illness, Scientific American, 273 (1995) 54-61.

[2] D.J. Temple, R. Ball, P.K. Weathersby, E.C. Parker, S.S. Survanshi, The Dive Profiles and Manifestations of Decompression Sickness Cases After Air and Nitrogen-Oxygen Dives. Volume I: Data Set Summaries, Manifestation Descriptions, and Key Files. NMRC 99-02(Vol. I), Naval Medical Research Center, Bethesda, MD, 1999.

[3] D.J. Temple, R. Ball, P.K. Weathersby, E.C. Parker, S.S. Survanshi, The Dive Profiles and Manifestations of Decompression Sickness Cases After Air and Nitrogen-Oxygen Dives. Volume II: Complete Profiles and Graphic Representations for DCS Events. NMRC 99-02(Vol II.), Naval Medical Research Center, Bethesda, MD, 1999.

[4] A.E. Boycott, G.C.C. Damant, J.S. Haldane, The Prevention of Compressed-Air Illness, Journal of Hygiene, 8 (1908) 342-443.

[5] P.K. Weathersby, L.D. Homer, E.T. Flynn, On the Likelihood of Decompression Sickness, Journal of Applied Physiology: Respiration Enviromental Exercise Physiology, 57 (1984) 815-825.

[6] T.E. Berghage, J.M. Woolley, L.J. Keating, The Probabilistic Nature of Decompression Sickness, Undersea Biomedical Research, 1 (1974) 189-196.

[7] P.K. Weathersby, W.A. Gerth, Survival Analysis and Maximum Likelihood Techniques as Applied to Physiological Modeling, in: P.K. Weathersby, W.A. Gerth (Eds.) Fifty-first Workshop of the Undersea and Hyperbaric Medical Society, Undersea and Hyperbaric Medical Society, 2002, pp. 1-40.

[8] H.D. Van Liew, E.T. Flynn, Decompression Tables and Dive-Outcome Data: Graphical Analysis, Undersea & Hyperbaric Med., 32 (2005) 184-198.

[9] E.C. Parker, S.S. Survanshi, P.K. Weathersby, E.D. Thalmann, Statistically Based Decompression Tables VIII: Linear-Exponential Kinetics. NMRI 92-73, Naval Medical Research Institute, Bethesda, MD, 1992.

[10] L.E. Howle, P.W. Weber, E.A. Hada, R.D. Vann, P.J. Denoble, The Probability and Severity of Decompression Sickness, PLOS ONE, 12 (2017).

[11] U.S. Department of Navy, U.S. Navy Diving Manual. Revision 7, Naval Sea Systems Command, Washington, D.C., 2016.

[12] R.D. Vann, P.J. Denoble, L.E. Howle, P.W. Weber, J.J. Freiberger, C.F. Pieper, Resolution and Severity in Decompression Illness, Aviation, Space, and Environmental Medicine, 80 (2009) 466-471.

[13] L.E. Howle, P.W. Weber, R.D. Vann, M.C. Campbell, Marginal DCS Events: Their Relation to Decompression and Use in DCS Models, Journal of Applied Physiology, 107 (2009) 1539-1547.

[14] F.G. Murphy, A.J. Swingler, W.A. Gerth, L.E. Howle, Iso-Risk Air No Decompression Limits After Scoring Marginal Decompression Sickness Cases as Non-Events, Computers in Biology and Medicine, 92 (2018) 110-117.

[15] A.E. King, N.R. Andriano, L.E. Howle, Trinomial Decompression Sickness Model using Full, Marginal, and Non-Event Outcomes, Computers in Biology and Medicine, 118 (2020).

[16] P.K. Weathersby, S.S. Survanshi, R.Y. Nishi, E.D. Thalmann, Statistically Based Decompression Tables VII: Selection and Treatment of Primary Air and N2O2 Data. NSMRL 1182/NMRI92-85, Joint Technical Report: Naval Submarine Medical Research Laboratory and Naval Medical Research Institute, Bethesda, MD, 1992.

[17] P.K. Weathersby, S.S. Survanshi, L.D. Homer, E. Parker, E.D. Thalmann, Predicting the Time of Occurrence of Decompression Sickness, Journal of Applied Physiology, 72 (1992) 1541-1548.

[18] A.E. King, F.G. Murphy, L.E. Howle, Bimodal Decompression Sickness Onset Times are Not Related to Dive Type or Event Severity, Computers in Biology and Medicine, 91 (2017) 59-68.

[19] E.D. Thalmann, E.C. Parker, S.S. Survanshi, P.K. Weathersby, Improved Probabilistic Decompression Model Risk Predictions Using Linear-Exponential Kinetics, Undersea and Hyperbaric Medical Society, 24 (1997) 255-274.
[20] L.E. Howle, Analytic Gain in Probabilistic Decompression Sickness Models, Computers in Biology and Medicine, 43 (2013) 1739-1747.
[21] L.E. Howle, P.W. Weber, R.D. Vann, A Computationally Advantageous System for Fitting Probabilistic Decompression Models to Empirical Data, Computers in Biology and Medicine, 39 (2009) 1117-1129.
[22] W.A. Gerth, Overview of Survival Functions and Methodology, in: P.K. Weathersby, W.A. Gerth (Eds.) Fifty-first Workshop of the Undersea and Hyperbaric Medical Society, Undersea and Hyperbaric Medical Society, Seattle, WA, 2002, pp. 1-48.
[23] L.E. Howle, P.W. Weber, J.M. Nichols, Bayesian Approach to Decompression Sickness Model Parameter Estimation, Computers in Biology and Medicine, 82 (2017) 3-11.
[24] Systat Software Inc, 2107 North First Street, Suite 360. San Jose, CA 95131.

This material is based upon work supported by the National Science Foundation Graduate Research Fellowship under Grant No. DGE-1644868 and by the U.S. Navy, Naval Sea Systems Command under contracts #N00024-13-C-4104 and #N00024-17-C-4317. Any opinion, findings, and conclusions or recommendations expressed in this material are those of the authors and do not necessarily reflect the views of the National Science Foundation or the U.S. Navy. Computational resources were provided by BelleQuant Engineering, PLLC. Neither funding agency nor the commercial entity played any role in designing this study, data collection and analysis, decision to publish, interpreting the results, or writing the manuscript.

The authors have no potential competing interests or financial or personal relationships that could inappropriately influence this work.

No authors have any conflicts of interest to disclose.